HHS Public Access

Author manuscript

J Am Chem Soc. Author manuscript; available in PMC 2023 March 22.

Published in final edited form as:

J Am Chem Soc. 2022 April 27; 144(16): 7085–7088. doi:10.1021/jacs.2c02404.

Exploiting Endogenous Enzymes for Cancer-Cell Selective Metabolic Labeling of RNA in Vivo

Samantha Beasley,
Department of Pharmaceutical Sciences, University of California—Irvine, Irvine, California 92697, United States

Abigail Vandewalle,
Department of Pharmaceutical Sciences, University of California—Irvine, Irvine, California 92697, United States

Monika Singha,
Department of Pharmaceutical Sciences, University of California—Irvine, Irvine, California 92697, United States

Kim Nguyen,
Department of Pharmaceutical Sciences, University of California—Irvine, Irvine, California 92697, United States

Whitney England,
Department of Pharmaceutical Sciences, University of California—Irvine, Irvine, California 92697, United States

Eric Tarapore,
Department of Developmental & Cellular Biology, University of California—Irvine, Irvine, California 92697, United States

Nan Dai,
New England Biolabs, Ipswich, Massachusetts 01938, United States

Ivan R. Corrêa Jr.,
New England Biolabs, Ipswich Massachusetts 01938, United States

Scott X. Atwood,
Department of Developmental & Cellular Biology, University of California—Irvine, Irvine, California 92697, United States

Robert C. Spitale
Department of Pharmaceutical Sciences and Department of Chemistry, University of California—Irvine, Irvine, California 92697, United States

rspitale@uci.edu .

Complete contact information is available at: https://pubs.acs.org/10.1021/jacs.2c02404

The authors declare no competing financial interest.

Supporting Information
The Supporting Information is available free of charge at https://pubs.acs.org/doi/10.1021/jacs.2c02404.
Experimental methods, synthetic schemes, and spectra for all compounds (PDF)

Abstract

Tissues and organs are composed of many diverse cell types, making cell-specific gene expression profiling a major challenge. Herein we report that endogenous enzymes, unique to a cell of interest, can be utilized to enable cell-specific metabolic labeling of RNA. We demonstrate that appropriately designed “caged” nucleosides can be rendered active by serving as a substrate for cancer-cell specific enzymes to enable RNA metabolic labeling, only in cancer cells. We envision that the ease and high stringency of our approach will enable expression analysis of tumor cells in complex environments.

Isolating and profiling RNA molecules from specified cells is a long-standing challenge in molecular biology. Metabolic labeling using nucleosides endowed with several types of chemical functional groups such as alkyne, azide, and more recently vinyl groups enable tracking and analysis by fluorescence or enrichment (Figure 1a).[1–5]

A major limitation with chemical approaches to track RNA expression is the inability to tag RNAs from cell types of interest. Expression of exogenous enzymes (Figure 1a) that, when paired with modified nucleosides/nucleobases, can enable cell-specific metabolic labeling of RNA.[6–11] However, each of these methods relies on expression of an exogenous enzyme, which requires laborious procedures to produce expression constructs; further, the utilization in living animals takes extensive time to implement. Overall, these limitations suggest additional methods need to be explored for cell-specific metabolic labeling of RNA, but may also present an opportunity for more sophisticated chemical approaches toward this problem.

An alternative approach, which has yet to be demonstrated, is utilizing endogenous enzymes to control metabolic labeling (Figure 1b). Unique cell types often use the expression of cell-specific enzymes to regulate signaling pathways that control cell functions such as cell motility, and metabolic activity to achieve maximal fitness.[12] The ability to develop novel chemical approaches for cell-specific metabolic labeling that do not require exogenous enzyme expression or cellular engineering not only would be incredibly useful for understanding cell-specific RNA expression but also could be seamlessly integrated with ongoing efforts in the field to utilize metabolic labeling to understand RNA–protein interactions,[13] RNA localization,[14–16] and even transcriptional dynamics.[17]

Herein, we present the synthesis and characterization of a novel metabolic reporter which is only metabolically incorporated into RNA in cancer cells. We envision this report will serve as a benchmark toward the development of enzyme-responsive metabolic reporters for measuring RNA expression within unique cell types and provide novel inroads toward utilizing chemical approaches to characterize gene expression within specific cancer cells.

Cancer cells are notorious for having unique enzyme expression and activity profiles to control growth and metastasis.[18,19] For example, histone deacetylases (HDACs) are known to be highly overexpressed and hyperactive in cancer cells to control gene expression.[20] Cathepsin proteases are another class of enzymes that are notoriously overexpressed in cancer cells, particularly metastatic cancers, to control degradation of the extracellular matrix and enable epithelial-to-mesenchymal transition (EMT) for subsequent metastases.[21]

These unique enzymatic signatures of cancer cells have been utilized for pro-drug approaches,[22] but have not been employed for metabolic labeling, and as such may provide inroads to distinguish cancer cell from normal cell RNA in complex tumor environments.

Our initial hypothesis was that we could achieve cancer-cell specific metabolic RNA labeling through the design of **Lys-2′N3A** (compd **1**; Figure 1b). **Lys-2′N3A** is designed to be an AND-gate (an AND-gate relies on two inputs to get a desired output) responsive nucleoside, needing both HDAC and Cathepsin L protease (CTSL) enzymes to "uncage" the N-6 protecting group to liberate **2′N3A** (compd **2**; Figure 1b). Therefore, our design should enable highly stringent cell-specific RNA metabolic labeling. A terminal acetylated amine would be a substrate for HDAC enzyme, liberating a lysine amine, which would serve as a substrate for CTSL cleavage. We have demonstrated previously the liberated product, **2′N3A**, is nontoxic in cells and yields robust RNA labeling.[7]

Lys2′N3A and **2′N3A** were synthesized in five steps starting with commercially available Vidarabine (Synthesis and Characterization in Supporting Information). Using high-performance liquid chromatography (HPLC), we demonstrated that **Lys-2′N3A** is a substrate and can be deacetylated by HDAC1, a broad spectrum HDAC enzyme,[22] and subsequently the N6-amide bond cleaved by CTSL. Deacylation of **Lys-2′N3A** is necessary for CTSL cleavage of the N6-amide (Figure S1; Supporting Information). These results suggest that **Lys-2′N3A** should be a substrate for dual activity of HDAC and CTSL enzymes in cells.

We next utilized an in-cell screening assay (Figure 2a) to determine if **Lys-2′N3A** would be preferentially incorporated into cancer cell RNA. Briefly, **Lys-2′N3A** was incubated in the media of either cancer or noncancer cells at 1 mM concentration for 24 h. Total RNA was harvested and biotinylated using CuAAC and alkyne biotin. Biotinylation was assessed using dot blot. We screened both cancerous and noncancerous cell lines. As shown in Figure 2b and c, we did not observe RNA incorporation above background in noncancer cell lines (Table S1). In contrast, we observed varying degrees of incorporation in cancer cell lines, with highly invasive cancers MDA-MB-231 and MCF7 (metastatic breast cancers), PC3 (pancreatic), or lung (LS174T) having very high incorporation into RNA. Interestingly, K562 cells (chronic myelogenous leukemia) did not have measurable incorporation of liberated **2′N3A**. This may be due to the nonmetastatic nature of such cancers, which do not undergo EMT and therefore would not have the need for expression of CTSL, undifferentiated state of the cells, or specificity of the patient line from which the line is derived. We also compared both **2′N3A** or **Lys-2′N3A** incubation for toxicity and using an MTT assay. We did not detect toxicity, consistent with our previous work using **2′N3A** for RNA metabolic labeling (Figure S2).[7] Concentration and time titration experiments revealed similar incorporation characteristics between **2′N3A** and **Lys-2′N3A** in the metastatic cancer line MDA-MB-231 (Figure S3). Control experiments demonstrate that we could not detect 2′N3A in cellular DNA by LC-MS/MS (Figure S4).

To further characterize the expression of HDAC and CTSL enzymes, we performed Western blot analysis for HDAC enzymes 1, 3, 4, 6, and 8, which represent a large portion of the complete HDAC class I and class II family of enzymes, as well as CTSL on cancer and

noncancerous lines (Figure S5). We observed more variability among cell lines (cancer and noncancer) for HDAC enzymes. Much higher signal was observed by Western for CTSL in MDA-MB-231 cells, with some observed in HeLa (Figure S5). We did not observe evidence of expression in HEK293 or K562 cells. Overall, these data suggest that “de-caging” of the Lys2′N3A is gated primarily by CTSL, but that HDAC expression is important for the liberation of the lysine substrate for CTSL cleavage.

We utilized known inhibitors of HDAC and CTSL enzymes to test if their incubation in cell media would decrease subsequent **2′N3A** incorporation into cellular RNA (Figure 2d). Trichostatin A is a broad inhibitor of HDAC activity. ZFY-CHO is a well-established specific inhibitor of cathepsin L activity. As demonstrated in Figure 2e and f and Figure S6, incubation of inhibitors at 0.2 mM and 0.5 mM with **Lys2′N3A** resulted in a marked decrease of incorporation of **2′N3A** into cellular RNA (see also Figure S6). These experiments support the notion that HDAC and CTSL decrease subsequent **2′N3A** incorporation into cellular RNA.

The utility of bio-orthogonal reporters can be demonstrated in cellular imaging. We also employed imaging to better understand the cell specificity of our metabolic labeling approach. We used cancerous (MDA-MB-231) and noncancerous (HEK293T) cells. As demonstrated in Figure S6, we observed that **Lys-2′N3A** is not incorporated into RNA noncancer cells even in coculture situations. These results further demonstrate the cell selectivity of cancer cell labeling for **Lys-2′N3A**.

We further aimed to test our approach in vivo. We established an in vivo xenograft tumor model of MDA-MB-231 cells (Figure 3a; Methods in Supporting Information). After 1 month, mice were subjected to an intraperitoneal injection of **2′N3A** or **Lys-2′N3A**. Organs were harvested and imaged using CuAAC. We observed bright fluorescence in the tumors of **Lys-2′N3A** injected animals, with a slight signal within the livers of the same animals (Figure 3b and c; Figure S7). In stark contrast, we observed fluorescence in the tumor and many organs with **2′N3A** injected animals (Figure 3d and e). Lastly, we treated tumor slices from both animals with RNase (Figure 3f) and observed a dramatic loss in signal, suggesting the signal was originating from RNA labeling. We isolated total RNA from organs and subjected isolated total RNA to biotinylation followed by analysis by dot blot. As shown in Figure 3g, RNA biotinylation profiles were similar to those observed in imaging experiments. Overall, these results suggest our strategy can selectively mark tumors using cell-selective metabolic labeling of RNA *in vivo*.

Herein, we have presented our efforts to develop novel chemical approaches to metabolically label RNA in complex environments. We have demonstrated that endogenous enzymes can be utilized to control metabolic labeling and achieve exquisite cell selectivity. We have further demonstrated that the specificity is achieved by two highly reactive enzymes in cancer cells, HDAC and CTSL, for precursor processing and eventual RNA labeling. Specificity was demonstrated not only in vitro through coculture systems but also in vivo, to mark tumor cells with high selectivity. We envision such an approach could be extended to other enzymes in the context of different diseases or specific organs in living animals. Further, probes such as the ones described here have potential to be employed

for transcriptome-wide analysis, as the azide functionality has been utilized for RNA biotinylation and enrichment in RNA sequencing workflows. Such directions are currently underway in our lab and will be reported in due course.

Supplementary Material

Refer to Web version on PubMed Central for supplementary material.

ACKNOWLEDGMENTS

We thank members of the Spitale lab for their careful reading and critique of the manuscript. This work is supported by the Ono Pharma Breakthrough Science Initiative Award to R.C.S. R.C.S. is a Pew Biomedical Scholar. S.B. is supported by an NIH training grant 5T32CA009054-40.

REFERENCES

(1). Gupta M; Singha M; Rasale DB; Zhou Z; Bhandari S; Beasley S; Sakr J; Parker SM; Spitale RC Mutually Orthogonal Bioconjugation of Vinyl Nucleosides for RNA Metabolic Labeling. Org. Lett 2021, 23 (18), 7183–7187. [PubMed: 34496205]

(2). Jao CY; Salic A. Exploring RNA transcription and turnover in vivo by using click chemistry. Proc. Natl. Acad. Sci. U. S. A 2008, 105 (41), 15779–84. [PubMed: 18840688]

(3). Kubota M; Nainar S; Parker SM; England W; Furche F; Spitale RC Expanding the Scope of RNA Metabolic Labeling with Vinyl Nucleosides and Inverse Electron-Demand Diels-Alder Chemistry. ACS Chem. Biol 2019, 14 (8), 1698–1707. [PubMed: 31310712]

(4). Nainar S; Beasley S; Fazio M; Kubota M; Dai N; Correa IR Jr.; Spitale RC Metabolic Incorporation of Azide Functionality into Cellular RNA. Chembiochem 2016, 17 (22), 2149–2152. [PubMed: 27595557]

(5). Zheng Y; Beal PA Synthesis and evaluation of an alkyne-modified ATP analog for enzymatic incorporation into RNA. Bioorg. Med. Chem. Lett 2016, 26 (7), 1799–802. [PubMed: 26927424]

(6). Hida N; Aboukilila MY; Burow DA; Paul R; Greenberg MM; Fazio M; Beasley S; Spitale RC; Cleary MD EC-tagging allows cell type-specific RNA analysis. Nucleic Acids Res. 2017, 45 (15), e138. [PubMed: 28641402]

(7). Miller MR; Robinson KJ; Cleary MD; Doe CQ TU-tagging: cell type-specific RNA isolation from intact complex tissues. Nat. Methods 2009, 6 (6), 439−41. [PubMed: 19430475]

(8). Nainar S; Cuthbert BJ; Lim NM; England WE; Ke K; Sophal K; Quechol R; Mobley DL; Goulding CW; Spitale RC An optimized chemical-genetic method for cell-specific metabolic labeling of RNA. Nat. Methods 2020, 17 (3), 311–318. [PubMed: 32015544]

(9). Nguyen K; Fazio M; Kubota M; Nainar S; Feng C; Li X; Atwood SX; Bredy TW; Spitale RC Cell-Selective Bioorthogonal Metabolic Labeling of RNA. J. Am. Chem. Soc 2017, 139 (6), 2148–2151. [PubMed: 28139910]

(10). Nguyen K; Kubota M; Arco JD; Feng C; Singha M; Beasley S; Sakr J; Gandhi SP; Blurton-Jones M; Fernandez Lucas J; Spitale RC A Bump-Hole Strategy for Increased Stringency of Cell-Specific Metabolic Labeling of RNA. ACS Chem. Biol 2020, 15 (12), 3099–3105. [PubMed: 33222436]

(11). Wang D; Zhang Y; Kleiner RE Cell- and Polymerase-Selective Metabolic Labeling of Cellular RNA with 2′-Azidocytidine. J. Am. Chem. Soc 2020, 142 (34), 14417–14421. [PubMed: 32786764]

(12). Sonawane AR; Platig J; Fagny M; Chen CY; Paulson JN; Lopes-Ramos CM; DeMeo DL; Quackenbush J; Glass K; Kuijjer ML Understanding Tissue-Specific Gene Regulation. Cell Rep 2017, 21 (4), 1077–1088. [PubMed: 29069589]

(13). Danan C; Manickavel S; Hafner M. PAR-CLIP: A Method for Transcriptome-Wide Identification of RNA Binding Protein Interaction Sites. Methods Mol. Biol 2022, 2404, 167–188. [PubMed: 34694609]

(14). Li Y; Aggarwal MB; Nguyen K; Ke K; Spitale RC Assaying RNA Localization in Situ with Spatially Restricted Nucleobase Oxidation. ACS Chem. Biol 2017, 12 (11), 2709–2714. [PubMed: 28952711]

(15). Engel KL; Lo HG; Goering R; Li Y; Spitale RC; Taliaferro JM Analysis of subcellular transcriptomes by RNA proximity labeling with Halo-seq. Nucleic Acids Res. 2022, 50 (4), e24. [PubMed: 34875090]

(16). Li R; Zou Z; Wang W; Zou P, Metabolic incorporation of electron-rich ribonucleosides enhances APEX-seq for profiling spatially restricted nascent transcriptome. Cell Chem. Biol 2022. DOI: 10.1016/j.chembiol.2022.02.005.

(17). Muhar M; Ebert A; Neumann T; Umkehrer C; Jude J; Wieshofer C; Rescheneder P; Lipp JJ; Herzog VA; Reichholf B; Cisneros DA; Hoffmann T; Schlapansky MF; Bhat P; von Haeseler A; Kocher T; Obenauf AC; Popow J; Ameres SL; Zuber J. SLAM-seq defines direct gene-regulatory functions of the BRD4-MYC axis. Science 2018, 360 (6390), 800–805. [PubMed: 29622725]

(18). Hanahan D; Weinberg RA Hallmarks of cancer: the next generation. Cell 2011, 144 (5), 646–74. [PubMed: 21376230]

(19). Hainaut P; Plymoth A. Targeting the hallmarks of cancer: towards a rational approach to next-generation cancer therapy. Curr. Opin Oncol 2013, 25 (1), 50–1. [PubMed: 23150341]

(20). Li Y; Seto E. HDACs and HDAC Inhibitors in Cancer Development and Therapy. Cold Spring Harb Perspect Med. 2016, 6 (10), a026831.

(21). Olson OC; Joyce JA Cysteine cathepsin proteases: regulators of cancer progression and therapeutic response. Nat. Rev. Cancer 2015, 15 (12), 712–29. [PubMed: 26597527]

(22). Ueki N; Lee S; Sampson NS; Hayman MJ Selective cancer targeting with prodrugs activated by histone deacetylases and a tumour-associated protease. Nat. Commun 2013, 4, 2735. [PubMed: 24193185]

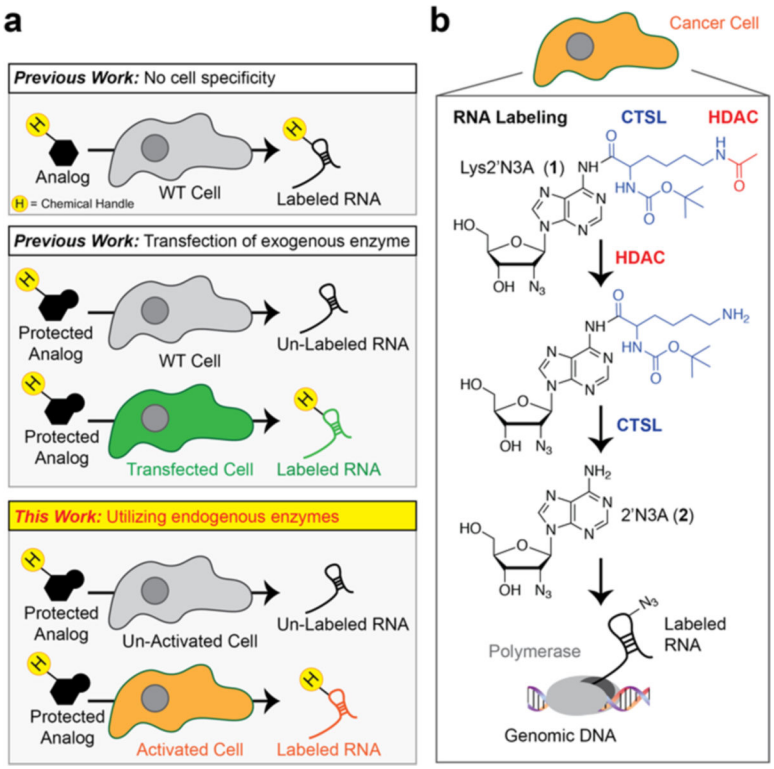

Figure 1.

Outline of cell-type specific metabolic labeling of RNA. (a) In metabolic labeling experiments, a chemically modified nucleoside analog is added to cells. The chemical modifications on the nucleobase/nucleoside analogs render them “inert” to endogenous metabolic pathways while the expression of specific metabolic enzymes can control their incorporation. Most studies to date rely on the overexpression of exogenous enzymes to control metabolic incorporation. (b) Our approach uses endogenous enzymes to “uncage” inert intermediates for eventual incorporation into RNA to apply cell-specific metabolic labeling of RNA in cancer cells. H = handle for conjugation such as alkyne or azide. HDAC = histone deacetylase. CTSL = cathepsin L protease.

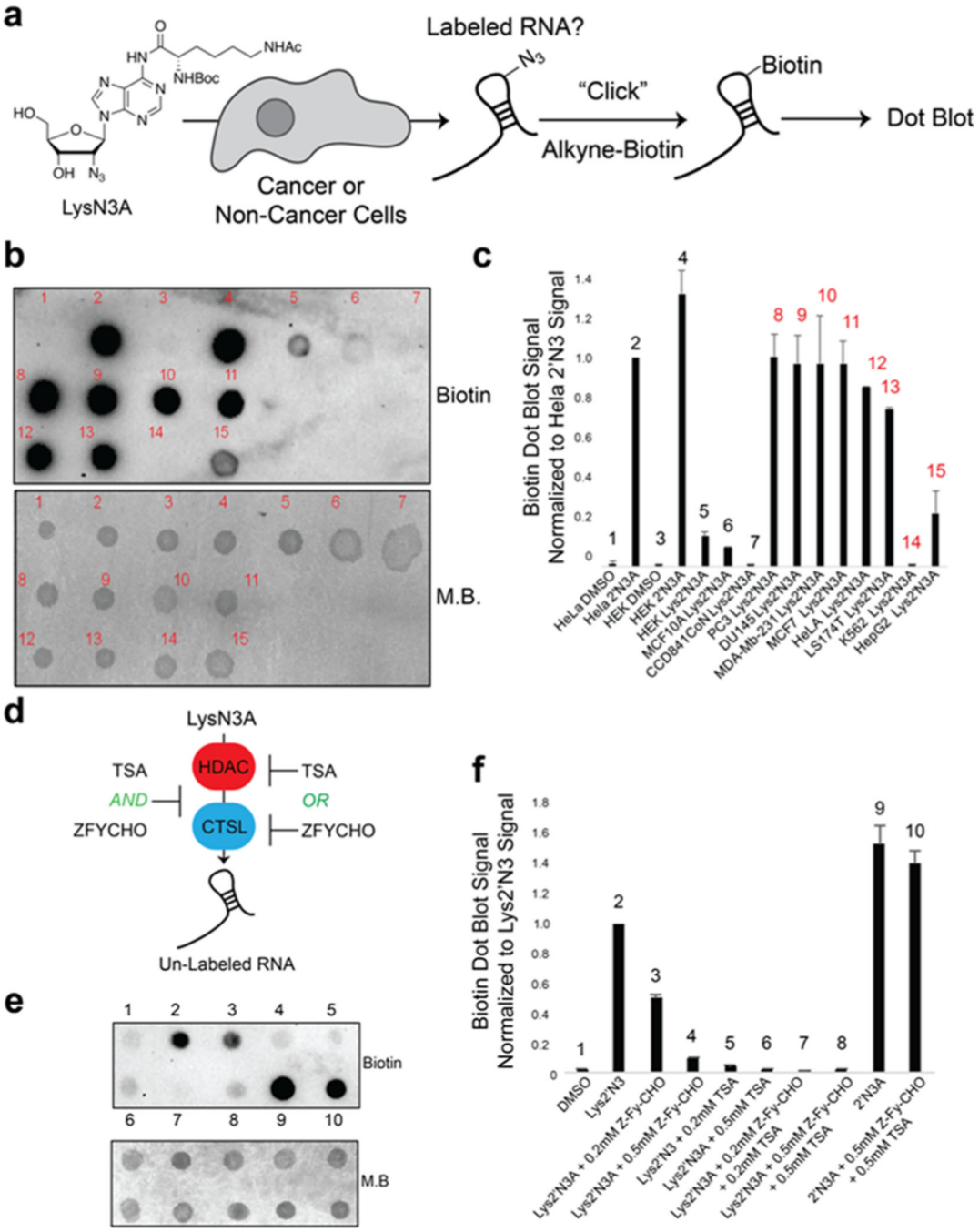

Figure 2.

Demonstration of cancer cell-specific metabolic labeling of RNA in cells. (a) Schematic of cell-based screen used for determining cell-specific metabolic labeling using **Lys2′N3A.** Cells were treated with 1 mM concentration of **Lys2′N3A** or **2′N3A** for 24 h. Total RNA was harvested and biotinylated using copper(I)-catalyzed azide−alkyne cycloaddition (CuAAC) with alkyne biotin. Biotinylation was assessed using dot blot. (b) Representative dot-blot analysis demonstrating that **Lys2′N3A** is only "uncaged" in cancer cells to enable **2′N3A** incorporation into RNA. M.B. = methylene blue dye to demonstrate loading onto

the dot blot membrane. Cell types are listed in Table S1. (c) Bar chart representing integrated signal from biological duplicate dot blots as in panel b. Red numbering above bar chart represents cancer types. Data were normalized to the **HeLa-2′N3A** dot blot sample. (d) Schematic of utilizing HDAC (histone deacetylase) and CTSL (cathepsin L protease) enzyme inhibitors to demonstrate their activity and 2′N3A incorporation into RNA. Cells were incubated with noted concentrations of inhibitors then treated with 0.2 mM final concentration and incubated for 5 h. RNA was then isolated and biotinylated for dot blot. (e) Representative dot blot analysis demonstrating that HDAC (histone deacetylase) and CTSL (cathepsin L protease) enzyme inhibitors suppress **Lys2′N3A** uncaging in HeLa cells. (f) Bar chart representing integrated signal from biological duplicate dot blots as in panel e. Data were normalized to the **HeLa-2′N3A** dot blot sample.

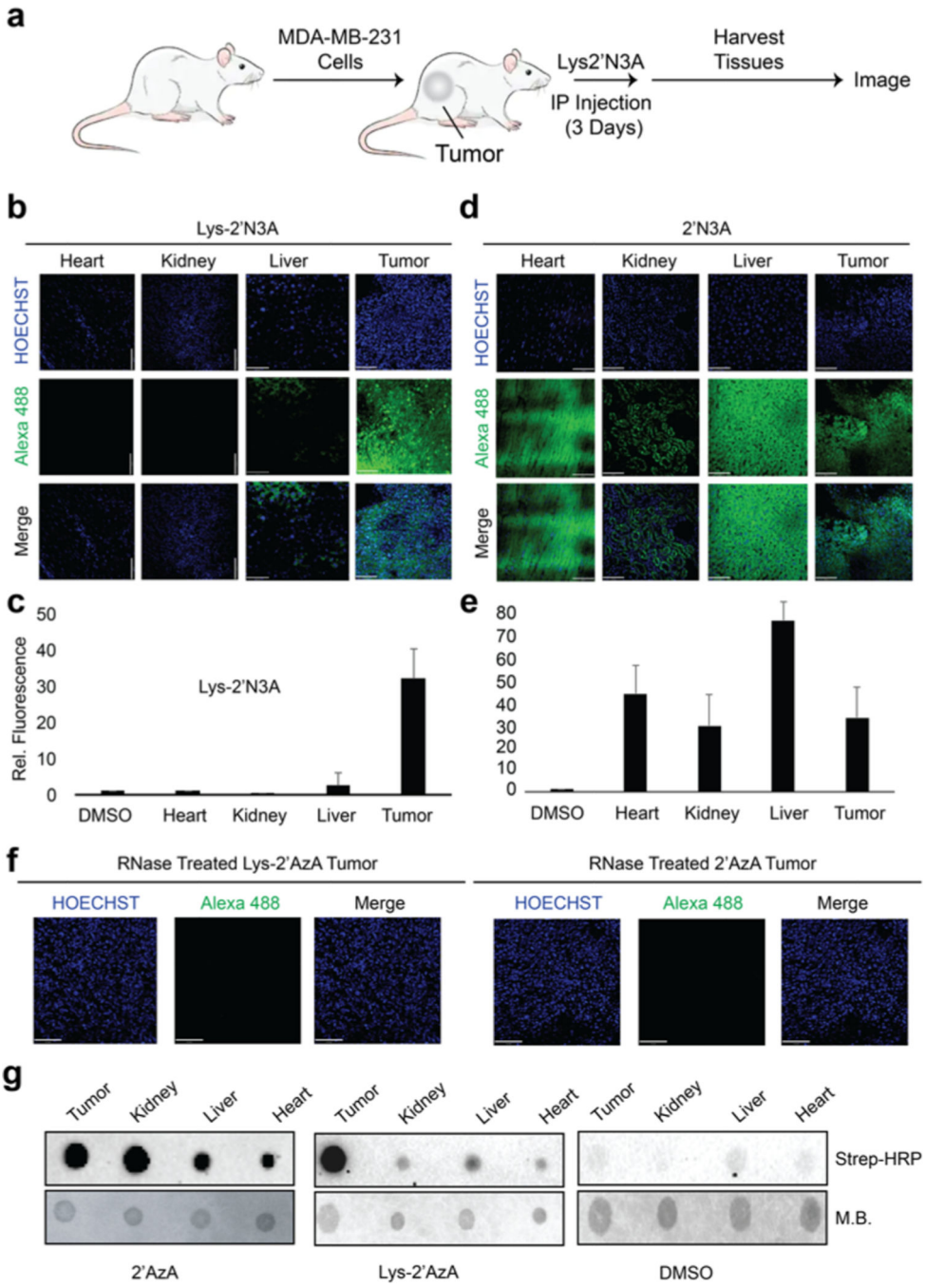

Figure 3.

Imaging cell-specific RNA labeling *in vivo*. (a) Outline of experiments used for RNA labeling in vivo. 100 μL of either DMSO, **2′N3A**, or **Lys2′N3A** were IP injected at a concentration of 2 mg/mL once per 24 h over 3 days. After 3 days, the mice were sacrificed, and the tumors and organs were collected and sectioned for imaging. (b) Imaging of isolated organs and tumor tissue from experiments exposing mice to **Lys2′N3A**. (c) Integration of fluorescence signal from slices represented in panel b. (d) Imaging of isolated organs and tumor tissue from experiments exposing mice to **2′N3A**. (e) Integration of fluorescence

signal from slices represented in panel d. (f) Imaging experiments demonstrating loss of fluorescent signal after RNase treatment. Sections were then incubated in a 0.2 mg/mL solution of RNase A in 0.5% Triton in 1× PBS pH 7.4 for 1 h, followed by 3× washes with DPBS. Slices were then imaged. (g) Dot blot on isolated RNA from various tissues following IP injection. IP injections were followed as described in panel a. Isolated RNA was then subjected to CuAAC with biotin alkyne. Dot blot was performed as in Figure 2. M.B. = methylene blue dye to demonstrate loading onto the dot blot membrane.